Angular Distribution of Sputtered Particles from Ternary Alloy $Fe_{71.9}Cr_{5.6}Al_{22.5}$ under Kr^+ Bombardment at Normal Incidence

A. Afkir[a], M. Ait El Fqih[a,b,*], A. El Boujlaidi[a], L. Jadoual[a], R. Jourdani[a], H. Aouchiche[c] and A. Kaddouri[a]

[a]Equipe Spectroscopie & Imagerie Atomiques des Matériaux, Université Cadi Ayyad, Marrakech, Maroc

[b]Laboratoire d'Ingénierie des Structures, Systèmes Intelligents et Energie Electrique, ENSAM; Université Hassan II, Casablanca, Maroc

[c]Laboratoire de Mécanique, Structures et Énergétique, Université Mouloud Mammeri de Tizi-Ouzou, BP 17, Tizi-Ouzou, Algeria

(Received July 17, 2018; in final form December 18, 2018)

Iron, chromium and aluminum particles sputtered under 5 keV by Kr^+ ion bombardment at normal incidence from the ternary alloy $Fe_{82}Cr_6Al_{12}$ was simulated. The Stopping and Range of Ions in Matter (SRIM) software combined to a new code-program, called *Angulaire*, were used to obtain the sputtering yields and angular distributions of the ejected species. The simulation was performed for a large number of incident ions (about 2×10^5 ions) and the number of particles emitted in the solid angle corresponding to the probe was counted by a computer. The angular distributions of sputtered particles were compared with the results available in the literature and showed a reasonable agreement. Furthermore, we have demonstrated that the angular distribution of the differential sputtering yields of all ejected species (iron, aluminum, and chromium) from the ternary alloy exhibited an over-cosine tendency.

DOI: 10.12693/APhysPolA.135.434

PACS/topics: sputtering yield, angular distribution, $Fe_{82}Cr_6Al_{12}$ ternary alloy

1. Introduction

It is known that many different mechanisms cause damages on the surface of solid matter, such as sputtering, blistering, and embrittlement. Sputtering is one of the occurring phenomena resulting from energetic ion beam and solid mater interactions. Sputtering of solid material induced by ions beam implies systematically ejection of particles when the energy of the beam exceeds the cohesive energy of the target. In addition, it is demonstrated that the major part of the ejected particles are neutral atoms in their ground state [1]. The angular distribution study of sputtered species from target components provides information about analytical models of sputtering phenomena, surface topography, target structure, and preferentially ejected particles [1, 2]. To our knowledge, the first investigations concerning the angular distributions are reported by Olson and Wehner [3] and Olson et al. [4] who revealed that the angular distributions of sputtered particles from binary alloys (Ag–Au, Cu–Ni, and Fe–Ni) have a dependence of sputtered flux composition on emission direction. Thus, after these pioneering works, numerous theoretical and experimental results under a wide variety of bombardment conditions were carried out on binary alloys in order to understand the angular spectra of sputtered atoms, ions, and molecules [5 ,6]. We would note here that, contrary to the binary alloys which are sufficiently studied theoretically and experimentally by several authors [7, 8], the available works in the literature on ternary alloys are scarce despite their wide use in different fields.

Besides, it is known that ternary alloys formed by iron, chromium, and aluminum have good oxidation and corrosion resistance at elevated temperatures due to their tendency to form a protective α-alumina layer, which are known to block the oxidation and corrosion processes [9, 10]. Furthermore, it is obvious that the amounts of chromium and aluminum needed in these materials to produce protective oxides at high oxygen pressures can be different from that needed at low oxygen partial pressures. Therefore, in the last decades, several researchers invested both theoretical and experimental effort to understand the behavior of these ternary alloys and the mechanisms that govern their properties [9–11].

The purpose of this work consists in a simulation study of the angular distribution of sputtered atoms of Fe, Cr, and Al from an iron–chromium–aluminum ($Fe_{82}Cr_6Al_{12}$ in atomic percent) amorphous ternary alloy under 5 keV Kr^+ beam bombardment at normal incidence. A new code-program, called Angulaire, was recently developed and then used for a refined treatment of the raw data obtained from the SRIM software. Note that the latter has already been tested by comparing it with the known OKSANA software [12] and with experimental results

*corresponding author; e-mail: m.aitelfqih@gmail.com

conducted by our team on Be at normal incidence [13] and on $Cu_{98}Be_2$ at different incidence angles [6]. In addition, an attempt to predict a semi-empirical law of the angular distribution of the sputtered particles is successfully achieved.

2. Simulation

2.1. SRIM-software

The SRIM software is a group of programs [14] that can predict how ions penetrate into an amorphous target and also the nuclear and electronic stopping power of these ions in the collisions cascade [15]. These collisions take into account the ion–atom interactions and are completed by a statistical algorithm of the Monte Carlo-type. The SRIM software provides information including the total sputtering yield as well as ion implantation into the target. One of the main approximations known in this software consists in the surface of the target which becomes smooth again after each ion impact. The simulations of the sputtered particles by 5 keV Kr^+ ion bombardment of an iron–chromium–aluminum alloy were carried out with the SRIM software. For a large number of incident ions (about 2×10^5 Kr^+ atoms), the ratios of Fe, Cr, and Al atoms emitted in the solid angle corresponding to each probe were counted. The SRIM software requires the introduction of several parameters; the cinematic conditions considered are that usually used in various experiments [16, 17]. The three remaining parameters are phenomenological ones, i.e. the energy barrier that the atom should overcome to be able to leave its site in the surface, the displacement energy corresponding to the atom movement (kinetic energy) and finally the surface energy barrier that the ejected atom should also overcome to be released. Once the calculation by the SRIM software is finished, a file containing all the raw results of the angular distributions in the form of cosine direction is automatically generated and saved. In the calculation, we do not take in the account the specific neighborhood of particles subjected to collisions.

2.1. Code-program Angulaire

The raw data obtained from the SRIM software are then processed by a new developed code-program, called Angulaire. Indeed, SRIM gives information only on the velocity of ejected particles and not on their numbers. Hence, an analytical treatment is undertaken through a mathematical formalism, via Angulaire, to find the sputtered particles. Besides, the cylindrical foil is subdivided in regular little squares forming a grid facilitating in this way the localization of the footprints of the sputtered particles. This program displays the image of the atoms ejected and deposited at the cylinder collector (the Mylar foil), and the spatial positions of the sputtered atoms on the grid; subsequently for each impact the numbers and type of atoms are written to an output file. The main introduced parameters are: the atomic number and the surface energy for each atom, the ratio of the radius of the cylinder collector on the side of the small square obtained from the subdivision of the simulated collector in its planar form (for more details see Fig. 2 in Ref. [6]), the number of columns (cutting lines) and finally the origin position ($x = 0$, $y = 0$) where the normal to the target crosses the collector (collector foil in a cylinder form).

2.2. Mathematical formalism

First of all, we introduce the grid cylinder in a suitable position surrounding the target. The cylinder axis is parallel to the surface of the target and normal to the plane of incidence. The geometry of the model is sketched in Fig. 1, where the different directions and angles are mentioned. We designate $\cos x$ as the ejection direction along

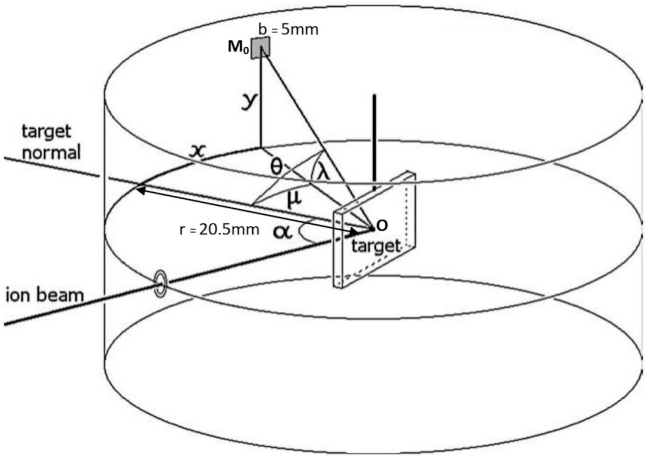

Fig. 1. Simulated collector geometry.

the x-axis such as that unit vector $\boldsymbol{u} = \boldsymbol{v}/v$, where v is the velocity of the ejected particles and $\boldsymbol{v}_0$ the (initial) ejection velocity when the particles leave the surface. It is the velocity of ejected particles changed on their way from target to collector, i.e. gas phase scattering is included in the system. The main physical quantity, here, is the direction of the velocity, $\boldsymbol{v}$, during the ejection of the particle. The velocity of the ejected particles in the frontier of the target in the z-direction is then given as $v_z^0 = \sqrt{2E_c^0/m}u_z^0$, where E_c^0 is the initial kinetic energy of the ejected particle, m — its mass and u_z^0 indicates its direction, designed $\cos(\theta)$ in the SRIM-software (see Fig. 2). Taking into account the surface energy E_s that the ejected particle should overcome, the quantity v_z^2 becomes

$$v_z^2 = \frac{2}{m}\left(E_c\left(u_z^0\right)^2 - E_s\right) \tag{1}$$

and then

$$v_z = \sqrt{\frac{2}{m}\left(E_c\left(u_z^0\right)^2 - E_s\right)}, \quad v_x = v_x^0 = \sqrt{\frac{2}{m}E_C^0}u_x^0,$$

$$v_y = v_y^0 = \sqrt{\frac{2}{m}E_C^0}u_y^0. \tag{2}$$

The components of the velocity can also be written as

$$v_x = ku_x^0, \quad v_y = ku_y^0, \quad v_z = k\sqrt{(u_z^0)^2 - \frac{E_s}{E_c^0}}$$

with

$$k = \sqrt{\frac{2}{m}E_C^0}. \tag{3}$$

Using the cylindrical coordinates (r, μ, z), an elementary solid angle $\mathrm{d}\Omega$ centered around a point M (see Fig. 1) can be written as

$$\mathrm{d}\Omega = \frac{\boldsymbol{OM}\cdot\boldsymbol{dS}}{OM^3} = \frac{r^2}{(r^2+z^2)}^{\frac{3}{2}}\,\mathrm{d}z\,\mathrm{d}u. \tag{4}$$

Note that the square side in the cylindrical (Mylar) foil is called b and the arc delimited by the square in the z-direction depends on the angle μ. We denote by z_0 the value of z at the center of the square, and by $\mu_0 = 0$ the value of μ at the center. The variation domain of the angle μ is then $[-b/(2r), +b/(2r)]$ and for z is: $[z_0 - b/2, z_0 + b/2]$. The solid angle Ω under which we see the square from point O can be written as

$$\Omega(z_0) = \int_{\frac{-b}{2r}}^{\frac{b}{2r}} \mathrm{d}u \int_{z_0-\frac{b}{2}}^{z_0+\frac{b}{2}} \mathrm{d}z \frac{r^2}{(r^2+z^2)^{\frac{3}{2}}}. \tag{5}$$

Furthermore, introducing the variable $\zeta = z/r$ we obtain:

$$\Omega(z_0) = \frac{b}{r}\int_{(z_0-b/2)/r}^{(z_0+b/2)/r} \frac{\mathrm{d}\zeta}{(1+\zeta^2)^{\frac{1}{3}}}. \tag{6}$$

With the given numerical values of cylindrical collector radius $r = 20.5$ mm and the square of deposited particles $b = 5$ mm, characterizing the cylinder considered, we obtain

$$\Omega(\zeta_0) = 0.238\left(\frac{\zeta_0 + 0.119}{\sqrt{1+(\zeta_0+0.119)^2}} - \frac{\zeta_0 - 0.119}{\sqrt{1+(\zeta_0-0.119)^2}}\right)$$

with

$$\zeta_0 = z_0/r. \tag{7}$$

Finally, to express Ω as a function of the emission angle θ defined between the axes Ox and OM_0, where M_0 is the center of the square considered, we use the relation $\zeta_0 = \tan\theta$.

3. Results and discussion

Figure 2a–c shows — in polar diagrams — the angular distributions of relative sputtering yields obtained from the iron–chromium–aluminum ternary alloy ($Fe_{82}Cr_6Al_{12}$) target under 5 keV krypton ion bombardments for a series of surfaces along the x-axis as a function of the solid angle Ω. In Fig. 2a–c, the full stars indicate the results of the simulated distributions, and the empty stars are those determined using the cosine fitting function: $F(\theta) = \frac{\partial Y(\theta)}{\partial\Omega} \propto \cos^n\theta$, where Y is sputtering yield, and the exponent n indicates the fit parameter. In the three cases considered, here, the yield is most important at lower angles and very small at the normal direction of emission as expected. Concerning the case where the ejected particles are iron (Fig. 2a), we note that the yield changes slightly from the emission angle 0° to 15°, and then its value becomes very sensitive to the emission angle, θ, beyond this angular range.

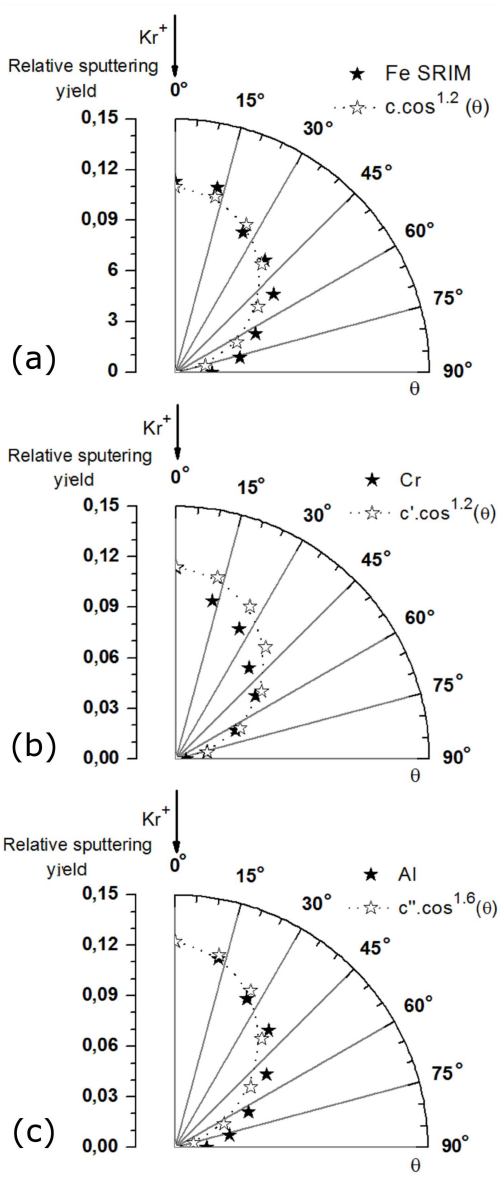

Fig. 2. Simulated angular distribution of sputter-ejected (a) Fe, (b) Cr and (c) Al, from $Fe_{82}Cr_6Al_{12}$ alloy target sputtered with 5 keV Kr^+ ions for a series of surfaces along the x-axis as a function of angle Ω. Dotted line is the best-fit curve.

In addition, the results obtained for the sputtering yield of each ejected species (iron, chromium, and aluminum) and the found values for the fit parameter n are given in Table I, where the corresponding highest ejection energy $E_{\max}$ is reported, too. Let us notice, first, that the yield has the most important value in the case of iron despite the greater value of the surface energy hampering the ejection of the particles. This can be explained easily by the abundance of the Fe (82% in atomic percent) in the ternary alloy used. Besides, the sputtering and the angular distribution of steel 316L irradiated by 4 keV helium ions were investigated by Emmoth et al. [18]. The sputtering yield determined experimentally for normal incidence was about 0.16 ± 0.03 atoms per incident ion. It is well known that, in this case, sputtering in the regime of linear cascades is not implemented. In our study, the simulated sputtering yields for He was 0.12 atoms per incident ion in accordance with that reported by Emmoth et al. [18]. The little discrepancy can be explained mainly by the surface roughness — facilitating the ejection of particles — which is not taken into account in the present simulation. In fact, it is well known that under ion beam bombardment leading to sputtering, the scanning electron micrographs of the irradiated samples revealed various modifications in the surfaces such as craters of typical size 10 μm with intertwined ripples [19, 20].

TABLE I

Best-fit n values from the fitting function $\cos^n\theta$ for Fe, Cr and Al in the $Fe_{82}Cr_6Al_{12}$ ternary alloy. Number of incident ions is 2×10^5

Targets↓	E_s [eV]	$E_{\max}$ [eV]	Y [atoms/ion]	Atomic percent [%]	n
Fe	4.34	2193.82	2.455	82	1.2
Cr	4.12	1849.595	0.804	6	1.2
Al	3.36	694.234	0.202	12	1.6

Furthermore, all the distribution curves exhibited an over-cosine tendency, with a fit parameter $n = 1.6$ for aluminum (Fig. 2c) and $n = 1.2$ for both iron and chromium (Fig. 2a and b, respectively). Emmoth et al. reported that the angular distribution was found to be wider than a cosine with $n = 0.7$ [18]. In another work on Al–Sn alloy (50% in wt%) under 27 keV Ar^+ bombardment at normal incidence, Wang et al. reported that $n = 1.22$ for the angular distribution of Sn atoms and $n = 1.07$ for that of the Al atoms [21]. It is important, here, to remind that the cascade linear-collision theory demands a cosine-type angular distribution, assuming a smooth and planar surface. However, previous experimental observations and computer simulations have established that over-cosine distribution is a rather general feature in the cascade regime [22, 23]. In the present simulation, we also observed an over-cosine angular distribution from the surface in the collision cascade region. The cause of these over-cosine distributions can be explained either by a surface-induced anisotropy in the recoil flux below the surface or by an anisotropic surface scattering recoil flux [6]. The statements on under and over cosine distributions can also be explained by simple geometrical considerations: for low ion energy (or mass, as for He) the collision cascade is shallow, i.e. close to the surface, and lateral ejection is likely, while for high ion energies, energy is mostly dissipated far below the surface, and only particles traveling on trajectories close to the surface (smallest distance from center of energy dissipation to surface) are ejected, hence the over-cosine distribution.

4. Conclusion

As concluding remarks, we have developed a code-program called Angulaire, combined with the SRIM software to describe the behavior of the sputtered particles under ion beam bombardment. Angular distributions of sputtered iron, chromium, and aluminum particles from an iron–chromium–aluminum ternary alloy ($Fe_{82}Cr_6Al_{12}$) were studied by computer simulation for the case of 5 keV krypton ions with the incidence direction of the ions along the normal to the sample surface. From the simulation using the new software, we have shown that the angular distribution exhibited an over-cosine tendency.

References

[1] W.O. Hofer, in: *Sputtering by Particle Bombardment III*, Eds. R. Behrisch, K. Wittmaack, Springer, Berlin 1991, p. 15.

[2] J.L. Whitton, *Ion Bombardment Modification of Surfaces: Fundamentals and Applications* Eds. O. Auciello, R. Kelly, Elsevier, Amsterdam 1984.

[3] R.R. Olson, G.K. Wehner, *J. Vac. Sci. Technol.* **14**, 319 (1977).

[4] R.R. Olson, M.E. King, G.K. Wehner, *J. Appl. Phys.* **50**, 3677 (1979).

[5] V.I. Shulga, *Nucl. Instrum. Methods Phys. Res. B* **164–165**, 733 (2000) and references therein.

[6] M. Ait El Fqih, P.-G. Fournier, *Acta Phys. Pol. A* **115**, 901 (2009).

[7] J. Dembowski, H. Oechsner, Y. Yamamura, M. Urbassek, *Nucl. Instrum. Methods Phys. Res. B* **18**, 464 (1987).

[8] J.P. Baxter, J.A. Schick, J. Sing, P.H. Kobrin, N. Winograd, *J. Vac. Sci. Technol. A* **4**, 1218 (1986).

[9] W.M. Lu, T.J. Pan, Y. Niu, *Oxid. Met.* **69**, 63 (2007).

[10] J. Engkvist, U. Bexell, M. Grehk, M. Olsson, *Mater. Corros.* **60**, 876 (2009).

[11] D. Orlicka1, N.J. Simms, T. Hussain J.R. Nicholls, *J. Mater. High Temp.* **32**, 167 (2015).

[12] P.-G. Fournier, A. Nourtier, V.I. Shulga, M. Ait El Fqih, *Nucl. Instrum. Meth. B* **230**, 577 (2005).

[13] M. Ait El Fqih, *Eur. Phys. J. D* **56**, 167 (2010).

[14] J.F. Ziegler, M.D. Ziegler, J.P. Biersack, *Nucl. Instrum. Methods Phys. Res. B* **268**, 1818 (2010).

[15] J.F. Ziegler, J.P. Biersack, U. Littmark, *The Stopping and Range of Ions in Solids*, Pergamon Press, New York 2003.

[16] A. El Boujlaidi, M. Ait El Fqih, K. Hammoum, H. Aouchiche, A. Kaddouri, *Eur. Phys. J. D* **66**, 273 (2012).

[17] A. El Boujlaidi, K. Hammoum, L. Jadoual, R. Jourdani, M. Ait El Fqih, H. Aouchiche, A. Kaddouri, *Nucl. Instrum. Meth. Phys. Res. B* **343**, 158 (2015).

[18] B. Emmoth, H. Bergsaker, C.H Wu, *J. Nucl. Mater.* **941**, 162 (1989).

[19] D. Ghose, S.B. Karmohapatro, *Adv. Electron. Electron Phys.* **79**, 73 (1990).

[20] A.M. Borisov, E.S. Mashkova, A.S. Nemov, *Vacuum* **73**, 65 (2004).

[21] Wang Zhenxia, Pan Jisheng, Zhang Jiping, Tao Zhenlan, *J. Mater. Sci. Let.* **11**, 719 (1992).

[22] C. Verdeil, T. Wirtz, H.-N. Migeon, H. Scherrer, *Appl. Surf. Sci.* **255**, 870 (2008).

[23] T. Aoyama, M. Tanemura, F. Okuyama, *Appl. Surf. Sci.* **351**, 100 (1996).